



# Response of X-1 Experiment Chamber to Target Explosions

R.R. Peterson and J.F. Santarius

June 1998

UWFDM-1088

Presented at the 13th Topical Meeting on the Technology of Fusion Energy, June 7-11, 1998, Nashville TN.

***FUSION TECHNOLOGY INSTITUTE***

***UNIVERSITY OF WISCONSIN***

***MADISON WISCONSIN***

### **DISCLAIMER**

This report was prepared as an account of work sponsored by an agency of the United States Government. Neither the United States Government, nor any agency thereof, nor any of their employees, makes any warranty, express or implied, or assumes any legal liability or responsibility for the accuracy, completeness, or usefulness of any information, apparatus, product, or process disclosed, or represents that its use would not infringe privately owned rights. Reference herein to any specific commercial product, process, or service by trade name, trademark, manufacturer, or otherwise, does not necessarily constitute or imply its endorsement, recommendation, or favoring by the United States Government or any agency thereof. The views and opinions of authors expressed herein do not necessarily state or reflect those of the United States Government or any agency thereof.

# **Response of X-1 Experiment Chamber to Target Explosions**

R.R. Peterson and J.F. Santarius

Fusion Technology Institute  
University of Wisconsin  
1500 Engineering Drive  
Madison, WI 53706

<http://fti.neep.wisc.edu>

June 1998

UWFDM-1088

Presented at the 13th Topical Meeting on the Technology of Fusion Energy, June 7–11, 1998, Nashville TN.

## RESPONSE OF X-1 EXPERIMENT CHAMBER TO TARGET EXPLOSIONS

R.R. Peterson  
University of Wisconsin, Fusion Technology Institute  
1500 Engineering Drive  
Madison, WI 53706 USA  
(608) 263-5646

J.F. Santarius  
University of Wisconsin, Fusion Technology Institute  
1500 Engineering Drive  
Madison, WI 53706 USA  
(608) 263-2685

### ABSTRACT

The X-1 pulsed power facility would drive targets that could release very intense x-rays, debris ions and neutrons. These target emissions must be contained in an experiment chamber that allows access for a variety of high energy density experiments, while confining the radioactive vapors and rubble produced in each experiment. A study is in progress to design and analyze the experiment chamber for X-1. The vaporization of chamber materials by target emissions is considered and the mechanical loading on chamber structures by the rapid vaporization is predicted and discussed.

### I. INTRODUCTION

The X-1 pulsed power facility is being designed to implode z-pinch plasmas and ICF capsules that would release intense pulses of x-rays, neutrons and debris.<sup>1</sup> The X-1 experiment chamber will be required to connect to the pulsed power efficiently, allow adequate experimental and diagnostics access, and contain radioactive vapor and rubble produced by the target explosions.

An important component of the design and analysis of the chamber is the response of chamber materials to target generated x-rays, neutrons and ion debris. An effort to design and analyze the X-1 experiment chamber is in progress at the University of Wisconsin. The design is evolving as X-1 requirements are being refined. The analysis effort includes target emission spectra, neutronics and radioactivity, response of materials to the target emissions and the resulting mechanical behavior, and chamber maintenance. This paper describes the response of experimental chamber materials to target emissions.

### II. X-1 EXPERIMENT CHAMBER

The X-1 experiment chamber concept is depicted in Figure 1. The design employs a "defense in depth" strategy. Multiple layers of protection are used to confine the blast generated by the energy contained in the chamber. The first level of protection is the

hemispherical mini-chamber<sup>2</sup> made of Kevlar with a graphite inner coating that it meant to stop the large pieces of magnetic debris, and most of the x-rays and debris ions emitted by the target. The mini-chamber may need replacement after shots with burning ICF targets, but it will be designed not to become a debris source itself. The next layer is an aluminum liner that will absorb those x-rays and debris ions that pass through holes in the mini-chamber. Both the liner and the mini-chamber will experience significant vaporization and melting. After a shot, the liner can be removed as a unit with the radioactive rubble trapped in inside. Fast-closing explosive valves will prevent radioactive debris from leaving the experiment chamber. In back of the liner is an aluminum structural wall to carry the impulsive and long-term pressure loading from the blast. Outside of the liner is a water shield to stop fusion neutrons and gamma rays emitted by radioactive materials.

Inside the chamber is a set of conical Magnetically Insulated Transmission Lines (MITL), which carry electrical current from the pulsed power at the edge of the target chamber. The interface between the MITLs and the pulsed power modules varies for the different pulsed power concepts for X-1. The long MITL concept (Figure 1) uses approximately 40 coaxial vacuum transmission lines to carry power to the experiment chamber. The vacuum and magnetic insulation make a transition to the conical MITLs at the chamber wall, where no insulator stack is required. The water transformer concept (not shown) uses transmission lines in water to carry the power to the chamber and an insulator stack prevents breakdown at the chamber wall and keeps water out of the chamber.

In this paper, the response of the mini-chamber, chamber liner and MITL and insulator stack to target explosions are discussed.

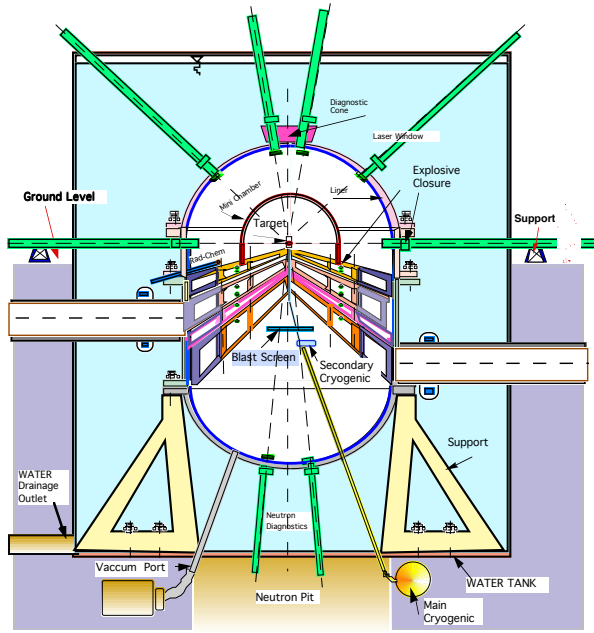


Figure 1. The X-1 experiment chamber concept.

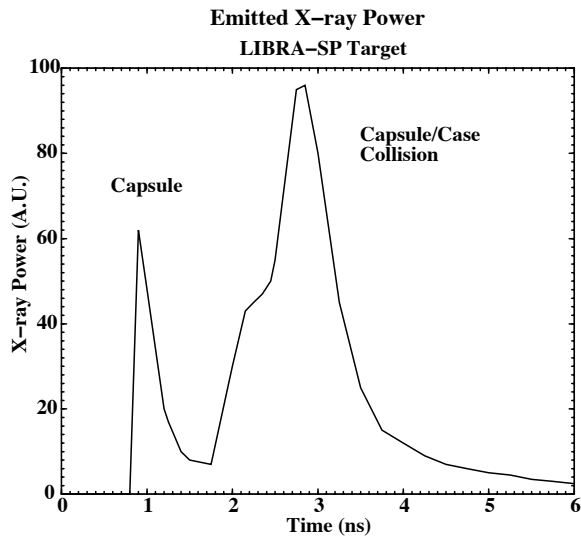


Figure 2. Emitted x-ray power from LIBRA-SP target.

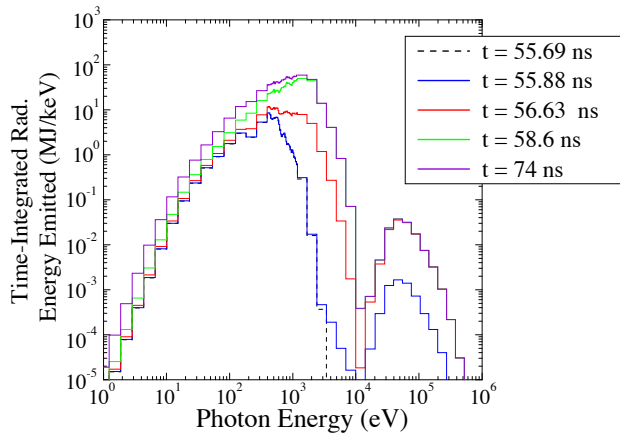


Figure 3. X-ray emission spectrum from LIBRA-SP target.

### III. TARGET EMISSIONS

The X-1 target will emit substantial energy in x-rays. X-rays are produced in a burning ICF target or by a z-pinch. In the X-1 target, the capsule expands at great speed ( $\approx 10^8$  cm/s), but because it is fully ionized x-ray emission is in Bremsstrahlung and only moderate. When the capsule collides with the gold hohlraum case and stagnates, the kinetic energy of the capsule is converted into internal energy of the gold/capsule mixture. This stagnated plasma radiates x-ray energy. Therefore, the x-ray emission power is the double pulse shown in Figure 2. The X-1 target x-ray spectrum will be mostly due to emission from the stagnated gold/capsule plasma. This emission is typically a blackbody spectrum at about 400 eV. There is some x-ray emission from the capsule that penetrates the gold hohlraum. The capsule is burning at a temperature of several tens of keV and gold has a reduced opacity around 50 keV. The spectra emitted by the LIBRA-SP light ion target<sup>3</sup>, integrated up to various times, are shown in Figure 3.

### IV. CALCULATIONAL MODEL

In the analysis of the blast response of the X-1 experimental chamber, the BUCKY computer code<sup>4</sup> has been used with equation-of-state and opacity data from SESAME<sup>5</sup> tables and EOSOPA<sup>6</sup> calculations. BUCKY is a 1-D Lagrangian radiation-hydrodynamics code in slab, cylindrical, and spherical geometry.

BUCKY models MHD effects and accepts thermal photon, laser, non-thermal x-ray, and ion external energy sources. BUCKY models thermonuclear burn with fusion product transport and is being used to study X-1 target implosions and burn. BUCKY can model phase changes in spherical, slab, and cylindrical solid or liquid regions adjacent to a plasma region. Energy is deposited on the surface of the solid or liquid region due to thermal conduction or thermal radiation from the plasma. X-ray and ion energy is deposited in the condensed matter volumetrically based on range-energy data. Thermal conduction in the liquid or vapor is calculated with temperature dependent thermal conductivities and heat capacities. Hydrodynamics is not modeled in solids or liquid regions, but when that material becomes vapor it joins the plasma region and the vapor moves into the plasma. If the condensed matter is modeled as part of a plasma region (SESAME and EOSOPA equations-of-state can include dense cold material), hydrodynamics can be calculated in solids or liquids, though the calculation of thermal conduction is not as accurate with this approach. BUCKY provides the time-dependent pressure and mass ablation rate on the surface of a material. The time-integrals of these give the impulse and total mass loss of

the material. Also, the energy remaining in the vapor after the vapor stops radiating leads to a quasi-steady-state pressure. This residual pressure applies a long-term load to the chamber that affects mechanical response. Assuming the vapor is an ideal gas, the residual pressure is 0.67 times the vapor energy per unit volume.

## V. MINI-CHAMBER

Using the analysis method described above, the responses of the X-1 1 m radius mini-chamber to the explosion of a 200 MJ target and 16 MJ of z-pinch x-rays have been calculated in spherical geometry. The results are summarized in Table 1 for the vaporization of graphite. The target and pinch x-ray photons vaporize graphite from the inside of the mini-chamber. The effects of the target ion debris are not included in the vaporization because they arrive at the mini-chamber later in time than the x-ray photons and they are absorbed in the blow-off vapor. Their energy contributes to the residual pressure but not to the recoil impulse on the structure. It has been observed that the vaporization follows the shape of the x-ray power curve. The residual pressure is 4.3 MPa, a substantial value. The vaporization leads to a recoil impulse of 136 Pa-s, which leads to significant vibrations in the mini-chamber.

The effects of magnetic debris are not yet analyzed. Magnetic debris energy fluences are of the same magnitude as x-rays and ion debris. The Kevlar in the main body of the mini-chamber is designed to absorb the energy of the magnetically accelerated projectiles without fracturing, though analysis of this phenomenon is needed.

The vaporization occurs over about 5 ns, too short a time for the vapor to move very far. So the vapor remains near solid for several ns. The vapor at 20 ns after the start of the x-ray pulse is still to a large degree within 100  $\mu\text{m}$  of the surface and the density on the surface is still about a tenth of solid density. Since a 200 MJ target explosion vaporizes about 10  $\mu\text{m}$ , this density is consistent with the vapor motion. The pressure of a vapor at solid density and a few eV is in the Mbar range, so the instantaneous pressure is very high. Integrating the pressure over several ns leads to a large recoil impulse on the surface of the structure, which is also equal to the product of the average velocity and the mass of the vapor.

The response of the mini-chamber of a non-yield shot with 16 MJ of z-pinch x-rays is similar to the response to a 200 MJ shot, with somewhat less vaporization. The same x-ray spectrum has been assumed and is scaled to 16 MJ. A parametric study of response versus yield has been performed and the results are shown in Figure 4. Once again the x-ray spectrum and pulse

shape discussed in section III are used and the photon fluence is scaled. It is seen that the response (peak pressure, impulse and mass vaporized) is close to linear in yield.

Table 1. Response of X-1 Mini-Chamber to Target Explosion

|  |                   |                   |
|--|-------------------|-------------------|
| Fusion Yield (MJ)                                  | 0                 | 200               |
| Mini-chamber Radius (cm)                           | 1.0               | 1.0               |
| X-ray Energy (MJ)                                  | 16                | 44                |
| X-ray Fluence ( $\text{J}/\text{cm}^2$ )           | 127               | 350               |
| Debris Ion Energy (MJ)                             | 0                 | 12                |
| Debris Ion Fluence ( $\text{J}/\text{cm}^2$ )      | 0                 | 95                |
| Magnetic Debris Energy (MJ)                        | 20                | 20                |
| Magnetic Debris Fluence ( $\text{J}/\text{cm}^2$ ) | 159               | 159               |
| Vapor Mass (kg)                                    | 0.142             | 0.247             |
| Impulse (Pa-s)                                     | 67                | 136               |
| Peak Pressure (MPa)                                | $2.3 \times 10^5$ | $6.2 \times 10^5$ |
| Residual Pressure (MPa)                            | 2.0               | 4.3               |

## VI. CHAMBER LINER

The response of the 2.5 m radius chamber liner is calculated in the same way as the mini-chamber. The mini-chamber has been removed in these calculations. There will be holes in the mini-chamber that allow x-rays and debris to reach the liner. These calculations put an upper limit on the damage caused by these target emissions because all x-rays and ions are assumed to leak through the mini-chamber. The results are summarized in Table 2, where results for no yield and 200 MJ and 1000 MJ are shown. The results are qualitatively similar to the mini-chamber results. As in the mini-chamber, debris ions only contribute to the residual pressure. Also, magnetic debris has yet to be considered. The results have been parametrically studied as a function of yield. Just as in the mini-chamber, the response is close to linear in target yield.

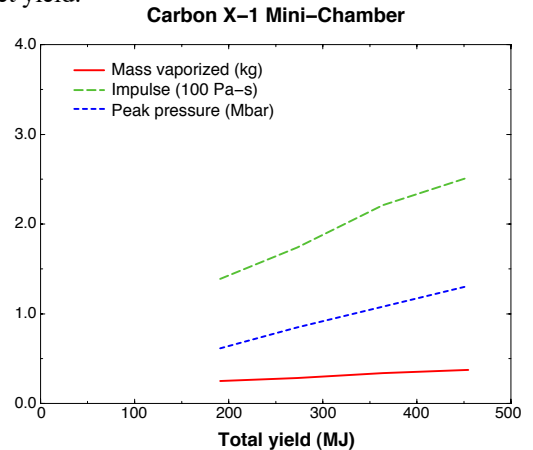


Figure 4. Mass vaporized, impulse and peak pressure on surface of X-1 mini-chamber as a function of target yield.

Table 2. Response of X-1 Chamber Liner to Target Explosion

|                                 |                   |                   |                   |
|---------------------------------|-------------------|-------------------|-------------------|
| Fusion Yield (MJ)               | 0                 | 200               | 1000              |
| Chamber Liner Radius            | 2.5               | 2.5               | 2.5               |
| X-ray Energy (MJ)               | 16                | 44                | 220               |
| X-ray Fluence ( $J/cm^2$ )      | 20.4              | 56.0              | 280               |
| Debris Ion Energy (MJ)          | 0                 | 12                | 61                |
| Debris Ion Fluence ( $J/cm^2$ ) | 0                 | 15                | 76                |
| Vapor Mass (kg)                 | 0.60              | 1.22              | 2.80              |
| Impulse (Pa-s)                  | 18.4              | 41.2              | 152               |
| Peak Pressure (MPa)             | $1.1 \times 10^5$ | $3.4 \times 10^5$ | $8.9 \times 10^5$ |
| Residual Pressure (MPa)         | 0.12              | 0.52              | 3.11              |

### VII. MITL AND INSULATOR STACK

The response of the plastic insulator stack to any portion of the target generated blast that propagates down the A-K gap in the MITLs is very important to the water transformer pulsed power option. Such a blast is assumed to be driven by the residual pressure in the mini-chamber, which somehow finds its way into the MITL gap. For a 200 MJ target explosion, the residual pressure in the mini-chamber is 4.3 MPa and the average carbon vapor density is  $58 \mu g/cm^3$ . A BUCKY simulation has been performed in cylindrical geometry for a 300 cm long MITL gap, which is initially at low pressure. The insulator stack is assumed to be at the end of the gap (Table 3). A substantial impulse and radiant fluence are applied to the insulator stack by the blast. Density profiles in the gap are shown in Figure 5 where the details of the rarefaction wave moving down the gap can be seen. Density begins to accumulate against the insulator stack, leading to a long-term pressure loading. This is seen in Figure 6 where the pressure and heat flux on the insulator stack are plotted against time. From these results, it is clearly possible to prevent this loading with a valve with a  $25 \mu s$  closing time if it is placed near the stack.

Table 3. Response of X-1 Insulator Stack to Blast Down MITL Gap

|                               |      |
|-------------------------------|------|
| Fusion Yield (MJ)             | 200  |
| Impulse (Pa-s)                | 154  |
| Peak Pressure (MPa)           | 0.44 |
| Radiated Fluence ( $J/cm^2$ ) | 94.5 |

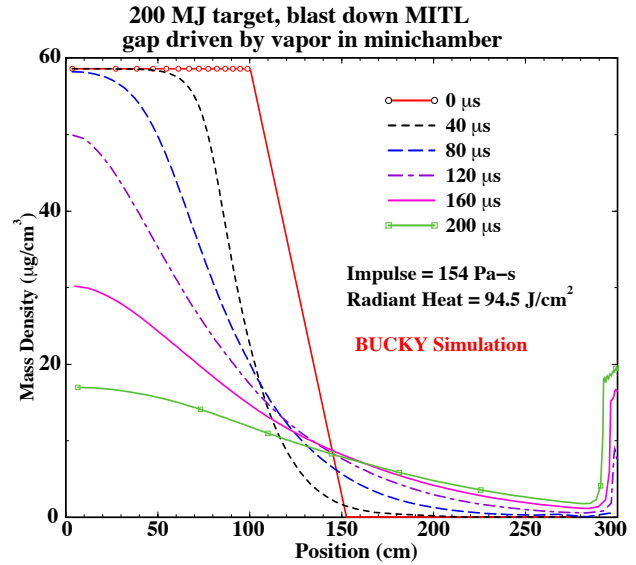


Figure 5. Density profiles in MITL gap from 200 MJ target explosion.

### VIII. SUMMARY AND CONCLUSIONS

The response of the experiment chamber to x-ray, ion and shrapnel loading is of great importance to the X-1 concept. Initial analysis has been performed that shows significant vaporization to experiment chamber materials. Additional analysis of the chamber concepts needs to be performed. To have confidence in the X-1 experiment chamber design, the methods of analysis need to be validated by experiments.

Additional analysis needs to be performed in the following areas:

1. One-dimensional chamber response for a broad range of likely target, z-pinch and magnetic debris loading. X-ray spectra specific to X-1 targets will become available in the near future and chamber analysis must be calculated using this information. Other target concepts for SBSS experiments will be shot in X-1 that will produce as yet unknown chamber environments. Response to high yield and unusual spectra must be considered. Z-pinch spectra will soon be available for X-1 and the responses to these x-rays need to be considered. This broad survey for responses to various targets should be performed initially in 1-D with the BUCKY code to find the worst conditions.

2. Two- and 3-D analysis of chamber response is needed to analyze the flow of vapor and dust into ports and gaps. The vapor and dust are radioactive and confinement schemes need to be analyzed in multiple dimensions.

3. Fragmentation and shrapnel need to be studied. Initial analytic models should be combined with 1-D BUCKY simulations to estimate shrapnel sizes and velocities. Models for fragmentation need to be developed and applied to these BUCKY simulations. Two- and 3-D fragmentation simulations need to be applied to X-1 conditions.

4. Flow of vapor and fragments needs to be calculated together in multi-phase simulations.

5. Melting of the liner needs to be analyzed.

6. Magnetic debris needs to be calculated with multi-D fragmentation codes.

Experimental validation needs to be done:

1. X-ray vaporization and melting experiments should be performed on Z or Saturn. The models in BUCKY need to be validated. Comparisons with measured impulses, vapor mass, melt mass, and fragment sizes are needed for BUCKY and fragmentation codes. Experiments need to be performed for all chamber materials (graphite lined Kevlar, aluminum alloy, steel).

2. Magnetic debris needs to be measured and compared with fragmentation code predictions.

3. Ion debris response needs to be validated with comparisons between RHEPP experiments and BUCKY predictions.

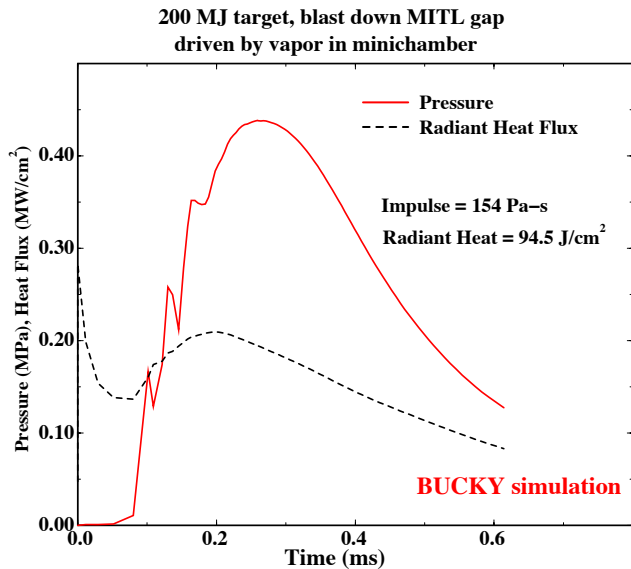


Figure 6. Pressure and heat flux on inner surface of X-1.

## ACKNOWLEDGMENT

This work has been supported by Sandia National Laboratories. E.A. Mogahed, I.N. Sviatoslavsky, G.L. Kulcinski, H.Y. Khater, M.E. Sawan and P. Cousseau of the University of Wisconsin have assisted in the X-1 design, as have G.E. Rochau, J.J. Ramirez, R.E. Olson, D. McDaniel, and many others at Sandia National Laboratories.

## REFERENCES

1. G.E. Rochau, J.J. Ramirez and P.S. Raglin, "Systems Analysis and Engineering of X-1 Advanced Radiation Source," these proceedings.
2. P.F. Peterson and J.M. Scott, "An Advanced Protection Concept for NIF", *Fusion Technology* 30, 442 (1996).
3. J.J. MacFarlane, M.E. Sawan, G.A. Moses, P. Wang, and R.E. Olson, "Numerical Simulations of the Explosion Dynamics and Energy Release from High-Gain ICF Targets," University of Wisconsin Fusion Technology Institute Report UWFD-1026 (June 1996).
4. J.J. MacFarlane, G.A. Moses, and R.R. Peterson, "BUCKY-1 – A 1-D Radiation Hydrodynamics Code for Simulating Inertial Confinement Fusion High Energy Density Plasmas," University of Wisconsin Fusion Technology Institute Report UWFD-984 (August 1995).
5. "SESAME: The Los Alamos National Laboratory Equation of State Database," LANL Report LA-UR-92-3407, edited by S.P. Lyon and J.D. Johnson (1992).
6. P. Wang, "ATBASE User's Guide", University of Wisconsin Fusion Technology Institute Report UWFD-984 (December 1993).